
Revisiting Membership Inference Under Realistic Assumptions

Bargav Jayaraman

Department of Computer Science
University of Virginia

Lingxiao Wang

Department of Computer Science
University of California Los Angeles

David Evans

Department of Computer Science
University of Virginia

Quanquan Gu

Department of Computer Science
University of California Los Angeles

Abstract

Membership inference attacks on models trained using machine learning have been shown to pose significant privacy risks. However, previous works on membership inference assume a balanced prior distribution where the adversary randomly chooses target records from a pool that has equal numbers of members and non-members. Such an assumption of balanced prior is unrealistic in practical scenarios. This paper studies membership inference attacks under more realistic assumptions. First, we consider skewed priors where a non-member is more likely to occur than a member record. For this, we use metric based on positive predictive value (PPV) in conjunction with membership advantage for privacy leakage evaluation, since PPV considers the prior. Second, we consider adversaries that can select inference thresholds according to their attack goals. For this, we develop a threshold selection procedure that improves inference attacks. We also propose a new membership inference attack called Merlin which outperforms previous attacks. Our experimental evaluation shows that while models trained without privacy mechanisms are vulnerable to membership inference attacks in balanced prior settings, there appears to be negligible privacy risk in the skewed prior setting.

1 Introduction

Differential privacy has become the gold standard for performing any privacy-preserving statistical analysis over sensitive data. The privacy and utility trade-off is controlled by the privacy loss budget parameter ϵ (and failure probability δ) such that smaller privacy loss budgets provide stronger privacy guarantees, whereas increasing budgets allows for more accurate results. Differentially private versions of many simple convex machine learning algorithms have been proposed in literature that consume a small privacy loss budget ($\epsilon < 1$) without sacrificing the model accuracy. These include empirical risk minimization algorithms such as logistic regression, linear regression and support vector machines [Chaudhuri et al., 2011, Zhang et al., 2012, Jain and Thakurta, 2013, Jayaraman et al., 2018]. Differentially private deep learning, however, still requires large ϵ values for performing meaningful learning. Some of the earlier works required ϵ in the order of hundreds [Zhao et al., 2018] to even millions [Shokri and Shmatikov, 2015]. Recent works have brought ϵ values down to single digits [Abadi et al., 2016, Beaulieu-Jones et al., 2018, Geyer et al., 2017, Bhowmick et al., 2018, Hynes et al., 2018] by exploiting theoretical advances in composition analysis of differential private mechanisms [Abadi et al., 2016, Dwork and Rothblum, 2016, Bun and Steinke, 2016, Mironov, 2017]. While it is inherent that larger privacy loss budgets lead to more leakage, it is still an open question how low privacy loss budgets should be to provide meaningful privacy in practice.

Differential privacy provides strong bounds on the worst-case privacy loss, but do not provide understanding of what privacy attacks could be realized in practice. Attacks, on the other hand, provide an empirical lower bound on privacy leakage for a particular setting. Many attacks on machine learning algorithms have been proposed that aim to infer private information about the model or the training data. These attacks include membership inference [Shokri et al., 2017, Long et al., 2017, Salem et al., 2019, Yeom et al., 2018], attribute inference [Fredrikson et al., 2014, 2015, Yeom et al., 2018], property inference [Ateniese et al., 2015, Ganju et al., 2018], model stealing [Lowd and Meek, 2005, Tramèr et al., 2016] and hyperparameter stealing [Wang and Gong, 2018, Yan et al., 2020]. Of these, membership inference and attribute inference attacks are most directly connected to the differential privacy definition and hence are a good basis for evaluating the privacy leakage of differentially private mechanisms. Essentially, if the privacy loss budget used is small enough, then the differentially private mechanism should be able to effectively defend against these attacks.

Several researchers have attempted to measure this privacy leakage empirically, including recent works by Rahman et al. [2018] and Jayaraman and Evans [2019]. Rahman et al. [2018] evaluate differentially private mechanisms against membership inference attacks and use accuracy and F-score as privacy leakage metrics. However, they do not specify the theoretical relationship between their privacy leakage metrics and the privacy loss budgets (i.e., how the metric would scale with increasing privacy loss budget) necessary to gain insight as to what privacy loss budgets are safe even in the worst case scenarios. Jayaraman and Evans [2019] evaluate the private mechanisms against both membership inference and attribute inference attacks using the advantage privacy leakage metric of Yeom et al. [2018]. This metric gives a theoretical upper bound based on the privacy loss budget, but it is not representative of true privacy leakage in realistic scenarios (as we demonstrate in Section 3). Both the above works consider a balanced prior data distribution probability and hence are not applicable to settings where the prior probability is skewed. Liu et al. [2019] theoretically evaluate differentially private mechanisms using a hypothesis testing framework using precision, recall and F-score metrics. They give a theoretical relationship connecting these metrics to the differential privacy parameters (ϵ and δ) and give some insights for choosing the parameter values based on the background knowledge of the adversary. Recently, Balle et al. [2019] provided hypothesis testing framework for analysing the relaxed variants of differential privacy that use Rényi divergence. However, neither of the above works provide empirical evaluation of privacy leakage of the private mechanisms. In another recent work, Farokhi and Kaafar [2020] propose to use the conditional mutual information as the privacy leakage metric and derive its upper bound based on KullbackLeibler divergence. Although they provide a relationship between this upper bound and the privacy loss budget, they do not evaluate the empirical privacy leakage in terms of the proposed metric. We provide theoretical analysis on privacy leakage metrics and perform membership inference attacks under two realistic assumptions. Namely, we consider prior data distribution probability and an adversary that can adaptively pick inference thresholds based on specific attack goals.

Theoretical Contributions. Motivated by these recent developments, we aim to develop more useful privacy metrics. Similarly to Liu et al. [2019], we adopt a hypothesis testing perspective on differential privacy in which the adversary uses hypothesis testing on the differentially private mechanism’s output to make inferences about its private training data. We use the recently proposed f -differential privacy notion (see Section 2.1) to bound the privacy leakage of the mechanism. Using this hypothesis testing framework, we tighten the theoretical bound on the advantage metric (Section 3.1). Then, we show that this metric alone does not suffice in most realistic scenarios since it does not consider the prior probability of the data distribution from which the adversary chooses records. We propose using positive predictive value (PPV) in conjunction with the advantage metric as it captures this notion, and provide a theoretical analysis of this metric (Section 3.2). We provide a threshold selection procedure to improve the existing inference attacks and also propose our novel inference attack that achieves higher PPV than the existing inference attacks (Section 4). Finally, we empirically evaluate the privacy leakage of differentially private neural network algorithms using both the metrics and find a smaller gap between theoretical and empirical leakage than the best found in prior work (Section 6), although the empirical leakage is still not high enough to pose a privacy threat. However, the non-private models are highly vulnerable to our inference attacks.

Summary of Findings. We perform an empirical evaluation of neural networks trained with and without differential privacy on three multi-class data sets considering balanced and imbalanced prior data distribution. The privacy leakage evaluation is performed via the loss-based attack of Yeom et al.

Notation	Description
$\mathcal{D} = \mathcal{X} \times \mathcal{Y}$	Distribution of records with features sampled from \mathcal{X} and labels sampled from \mathcal{Y}
$S \sim \mathcal{D}^n$	Data set S consisting of n records, sampled i.i.d. from distribution \mathcal{D}
$\mathbf{z} \sim S$	Record \mathbf{z} is picked uniformly random from data set S
$\mathbf{z} \sim \mathcal{D}$	Record \mathbf{z} is chosen according to the distribution \mathcal{D}
\mathcal{M}_S	Model obtained by using a learning algorithm \mathcal{M} over data set S
\mathcal{A}	Membership inference adversary
p	Probability of sampling a record from training set
γ	Test-to-train set ratio, $(1 - p)/p$
ϵ	Privacy loss budget of DP mechanism
δ	Failure probability of DP mechanism
α	False positive rate of inference adversary
β	False negative rate of inference adversary
ϕ	Decision threshold of inference adversary; also called rejection rule in hypothesis testing
Φ	Cumulative distribution function of standard normal distribution

Table 1: Notation

[2018], called Yeom, and our proposed Merlin attack (see Section 4.2). The results (Sections 6 and 7) corroborate our claims:

- Non-private models are highly vulnerable to inference attacks in the balanced prior setting.
- PPV decreases as the prior gets more skewed and hence it is a more reliable metric in imbalanced prior settings.
- Merlin achieves higher PPV than Yeom, and is a more effective attack in the settings that matter most.
- Private models are not vulnerable to any of the attacks even for privacy loss budgets well above the theoretical guarantees.

2 Differential Privacy

This section provides background on the differential privacy notions we use. Table 1 summarizes the notations we use throughout.

Dwork et al. [2006] introduced a formal notion of privacy that provides a probabilistic information-theoretic security guarantee:

Definition 2.1 (Differential Privacy). A randomized algorithm \mathcal{M} is (ϵ, δ) -differentially private if for any pair of neighbouring data sets S, S' that differ by one record, and any set of outputs O ,

$$Pr[\mathcal{M}(S) \in O] \leq e^\epsilon Pr[\mathcal{M}(S') \in O] + \delta.$$

Thus, the ratio of output probabilities across neighbouring data sets is bounded by the ϵ and δ parameters. The intuition behind this definition is to make any pairs of neighbouring data sets indistinguishable to the adversary given the information released.

From a hypothesis testing perspective [Wasserman and Zhou, 2010, Kairouz et al., 2017, Liu et al., 2019, Balle et al., 2019, Dong et al., 2019], the adversary can be viewed as performing the following hypothesis testing problem given the output of either $\mathcal{M}(S)$ or $\mathcal{M}(S')$:

H_0 : the underlying data set is S ,

H_1 : the underlying data set is S' .

According to the definition of differential privacy, given the information released by the private algorithm \mathcal{M} , the hardness of this hypothesis testing problem for the adversary is measured by the worst-case likelihood ratio between the distributions of the outputs $\mathcal{M}(S)$ and $\mathcal{M}(S')$. Following Dong et al. [2019], a more natural way to characterize the hardness of this hypothesis testing problem is its type I and type II errors and can be formulated in terms of finding a rejection rule ϕ which trades off between type I and type II errors in an optimal way. In other words, for a fixed type I error

α , the adversary tries to find a rejection rule ϕ that minimizes the type II error β . More specifically, recalling the definition of trade-off function proposed in Dong et al. [2019]:

Definition 2.2 (Trade-off Function). For any two probability distributions P and Q on the same space, the *trade-off function* $T(P, Q) : [0, 1] \rightarrow [0, 1]$ is defined as:

$$T(P, Q)(\alpha) = \inf\{\beta_\phi : \alpha_\phi \leq \alpha\},$$

where the infimum is taken over all (measurable) rejection rules, and α_ϕ and β_ϕ are the type I and type II errors for the rejection rule ϕ .

This definition suggests that the larger the trade-off function is, the harder the hypothesis testing problem will be. It has been established in Dong et al. [2019] that a function $f : [0, 1] \rightarrow [0, 1]$ is a trade-off function if and only if it is convex, continuous, non-increasing, and $f(x) \leq 1 - x$ for $x \in [0, 1]$. Thus, differential privacy can be reformulated as finding the trade-off function f that limits the adversary's hypothesis testing power, i.e., it maximizes the adversary's type II error for any given type I error.

2.1 f -Differential Privacy

The hypothesis testing formulation of differential privacy described above leads to the notion of f -differential privacy [Dong et al., 2019] (f -DP) which aims to find the optimal trade-off between type I and type II errors and will be used to derive the theoretical upper bounds of our proposed metrics for the privacy leakage.

Definition 2.3 (f -Differential Privacy). Let f be a trade-off function. A mechanism \mathcal{M} is f -differentially private if for all neighbouring data sets S and S' :

$$T(\mathcal{M}(S), \mathcal{M}(S')) \geq f.$$

Note that in the above definition, we abuse the notations of $\mathcal{M}(S)$ and $\mathcal{M}(S')$ to represent their corresponding distributions. For an (ϵ, δ) -differentially private algorithm, the trade-off function $f_{\epsilon, \delta}$ is given by Lemma 2.4 (proved by Wasserman and Zhou [2010] and Kairouz et al. [2017]):

Lemma 2.4 (Wasserman and Zhou [2010], Kairouz et al. [2017]). Suppose \mathcal{M} is an (ϵ, δ) -differentially private algorithm, then for a false positive rate of α , the trade-off function is:

$$f_{\epsilon, \delta}(\alpha) = \max\{0, 1 - \delta - e^\epsilon \alpha, e^{-\epsilon}(1 - \delta - \alpha)\}.$$

This lemma suggests that higher values of $f_{\epsilon, \delta}(\alpha)$ correspond to more privacy and perfect privacy would require $f_{\epsilon, \delta}(\alpha) = 1 - \alpha$. In addition, increasing ϵ and δ decreases $f_{\epsilon, \delta}(\alpha)$, reflecting the expected reduction in privacy.

2.2 Gaussian Differential Privacy

The Gaussian mechanism is one of the most popular and fundamental approaches for achieving differential privacy, especially for differentially private deep learning [Abadi et al., 2016]. Noisy stochastic gradient descent (SGD) and noisy Adam [Andrew et al., 2019], i.e., adding Gaussian noise (Gaussian mechanism) to SGD and Adam, are often used as the underlying private optimizers for training neural networks with privacy guarantees. Precisely characterizing the privacy loss of the composition of Gaussian mechanisms and deriving its sub-sampling amplification results, leads to the notion of Gaussian differential privacy [Dong et al., 2019], which belongs to the family of f -DP with a single parameter μ that defines the mean of the Gaussian distribution.

Definition 2.5 (μ -Gaussian Differential Privacy). A mechanism \mathcal{M} is μ -Gaussian differentially private if for all neighbouring data sets S and S' :

$$T(\mathcal{M}(S), \mathcal{M}(S')) \geq G_\mu,$$

where $G_\mu = T(\mathcal{N}(0, 1), \mathcal{N}(\mu, 1))$.

In this definition, G_μ is a trade-off function and hence μ -GDP is identical to f -DP where $f = G_\mu$. Lemma 2.6, which is established in Dong et al. Dong et al. [2019], gives the equation for computing G_μ :

Lemma 2.6. Given that \mathcal{M} is a μ -Gaussian differentially private algorithm, then for a false positive rate of α , the trade-off function is given as:

$$G_\mu(\alpha) = \Phi(\Phi^{-1}(1 - \alpha) - \mu),$$

where Φ is the cumulative distribution function of standard normal distribution.

The Gaussian mechanism for μ -GDP is given by the following theorem [Dong et al., 2019].

Theorem 2.7. A mechanism \mathcal{M} operating on a statistic θ is μ -GDP if $\mathcal{M}(S) = \theta(S) + \zeta$, where $\zeta \sim \mathcal{N}(0, \nabla(\theta)^2/\mu^2)$ and $\nabla(\theta)$ is the global sensitivity of θ .

We also have the relationship between μ -GDP and (ϵ, δ) -DP as follows (Corollary 2.13 in Dong et al. [2019] and Theorem 8 in Balle and Wang [2018]):

Proposition 2.8. A mechanism is μ -GDP if and only if it is $(\epsilon, \delta(\epsilon))$ -DP for all $\epsilon \geq 0$, where

$$\delta(\epsilon) = \Phi\left(-\frac{\epsilon}{\mu} + \frac{\mu}{2}\right) - e^\epsilon \Phi\left(-\frac{\epsilon}{\mu} - \frac{\mu}{2}\right).$$

Gaussian differential privacy supports lossless composition of mechanisms (Corollary 3.3 in Dong et al. [2019]) and privacy amplification due to sub-sampling (Theorem 4.2 in Dong et al. [2019]).

Theorem 2.9 (Composition). The T -fold composition of μ_i -GDP mechanisms is $\sqrt{\mu_1^2 + \dots + \mu_T^2}$ -GDP.

Theorem 2.10 (Sub-sampling). Suppose \mathcal{M} is f -DP on \mathcal{D}^m , if we apply \mathcal{M} to a subset of samples with sampling ratio $\tau = m/n \in [0, 1]$, then \mathcal{M} is $\min\{f_\tau, f_\tau^{-1}\}^{**}$ -DP, where $f_\tau = \tau f + (1 - \tau)Id$.

The function Id is the identity function defined as $Id(x) = 1 - x$, and $\min\{f_\tau, f_\tau^{-1}\}^{**}$ is the double conjugate of $\min\{f_\tau, f_\tau^{-1}\}$ function. Theorems 2.7, 2.9 and 2.10 can be combined to achieve GDP for gradient perturbation based machine learning algorithms such as noisy SGD and noisy Adam. For instance, adding standard Gaussian noise with standard deviation σ to each batch of gradients sampled with probability τ would lead to $\tau\sqrt{T}(e^{1/\sigma^2} - 1)$ -GDP for T compositions [Bu et al., 2019]. In our experiments, we use such result to characterize the privacy loss of our private optimizers for training differentially private neural networks, and use Proposition 2.8 to convert it into (ϵ, δ) -DP for the purpose of comparison.

3 Measuring Privacy Leakage

To evaluate privacy leakage, we define an adversarial game inspired by Yeom et al.'s Yeom et al. [2018]. Unlike their game which assumes a balanced prior, our game factors in the prior membership distribution probability. The adversarial game models the scenario where an adversary has access to a model, \mathcal{M}_S , trained over a data set S , knowledge of the training procedure and data distribution, and wishes to infer whether a given input is a member of that training set.

Experiment 3.1 (Membership Experiment). Assume a membership adversary, \mathcal{A} , who has information about the training data set size n , the distribution \mathcal{D} from which the data set is sampled, and the prior membership probability p . The adversary runs the following experiment:

1. Sample a training set $S \sim \mathcal{D}^n$ and train a model \mathcal{M}_S over the training set S .
2. Randomly sample $b \in \{0, 1\}$, such that $b = 1$ with probability p .
3. If $b = 1$, then sample $\mathbf{z} \sim S$; otherwise sample $\mathbf{z} \sim \mathcal{D} \setminus S$.
4. Output 1 if $\mathcal{A}(\mathbf{z}, \mathcal{M}_S, n, \mathcal{D}) = b$; otherwise output 0.

This membership experiment has two notable differences from the setting of Yeom et al. Yeom et al. [2018]. First, we consider a stronger adversary that differentiates a member of training set ($\mathbf{z} \sim S$) from a non-member ($\mathbf{z} \sim \mathcal{D} \setminus S$), as opposed to differentiating a member ($\mathbf{z} \sim S$) from the general data distribution ($\mathbf{z} \sim \mathcal{D}$). Second, our experiment incorporates the prior probability p of sampling a record, compared to the setting of Yeom et al. that assumes balanced prior probability ($p = 0.5$).

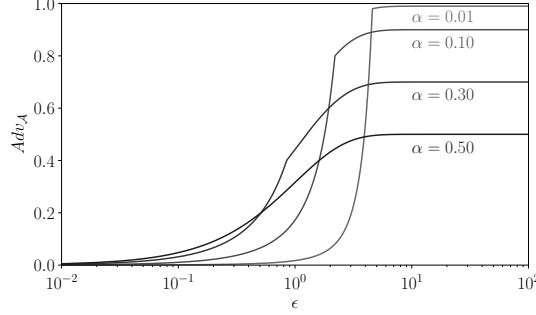


Figure 1: Theoretical upper bounds on $Adv_{\mathcal{A}}(\alpha)$ metric for various privacy loss budgets with varying α ($\delta = 10^{-5}$).

For most practical scenarios (that is, where being exposed as a member carries meaningful risk to an individual), p is much smaller than 0.5. For instance, considering the scenario of an epidemic outbreak, the training set could be the list of patients with the disease symptoms admitted at a hospital, or a group of hospitals. The non-members can be the remaining population of the city or a district. Hence, assuming a balanced prior of $p = 0.5$ is not a realistic assumption, and it is important to develop a privacy metric that can be used to evaluate scenarios with lower priors.

3.1 Membership Advantage

The membership advantage metric, Adv , was defined by Yeom et al. [2018] as the difference between the true positive rate and the false positive rate for the membership inference adversary provided that $p = 0.5$ (i.e., balanced prior membership distribution). Yeom et al. [2018] showed that for an ϵ -differentially private mechanism, the theoretical upper bound for membership advantage is $e^\epsilon - 1$, which can be quite loose for higher ϵ values and is not defined for $e^\epsilon - 1 > 1$ since the membership advantage metric proposed by Yeom et al. [2018] is only defined between 0 and 1. Moreover, the bound is not valid for (ϵ, δ) -differentially private algorithms which are more commonly used for private deep learning.

We derive a tighter bound for the membership advantage metric that is applicable to (ϵ, δ) -differentially private algorithms based on the notion of f -DP:

Theorem 3.1. Let \mathcal{M} be an (ϵ, δ) -differentially private algorithm. For any randomly chosen record \mathbf{z} and fixed false positive rate α , the membership advantage of a membership inference adversary \mathcal{A} is bounded by:

$$Adv_{\mathcal{A}}(\alpha) \leq 1 - f_{\epsilon, \delta}(\alpha) - \alpha,$$

where $f_{\epsilon, \delta}(\alpha) = \max\{0, 1 - \delta - e^\epsilon \alpha, e^{-\epsilon}(1 - \delta - \alpha)\}$.

Proof of Theorem 3.1. The proof follows directly from Yeom et al.'s definition, $Adv_{\mathcal{A}}(\alpha) = TPR - FPR$ when we have balanced prior membership distribution, $p = 0.5$. For a given $FPR = \alpha$, we have $1 - TPR \geq f_{\epsilon, \delta}(\alpha)$ according to the definition of trade-off function (Definition 2.2 and Lemma 2.4). Therefore, $Adv_{\mathcal{A}}(\alpha) \leq 1 - f_{\epsilon, \delta}(\alpha) - \alpha$. \square

Figure 1 shows the relationship between the false positive rate α of a given membership inference adversary and the upper bound of the advantage given by Theorem 3.1. This bound lies strictly between 0 and 1 and is tighter than the bound of Yeom et al. [2018], as shown in Figure 2. However, this metric is limited to balanced prior distribution of data and hence can overestimate (or underestimate) the privacy threat in any scenario where the prior probability is not 0.5. Thus, membership advantage alone is not a reliable way to measure the privacy leakage. Hence, we next propose the positive predictive value metric that considers the prior distribution of data.

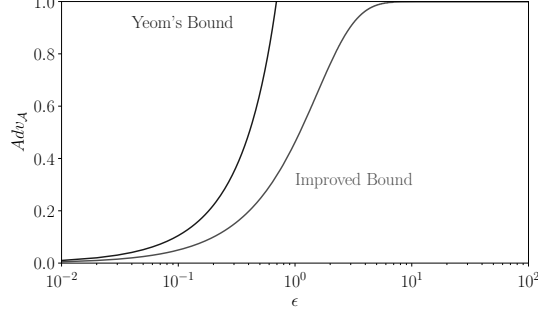


Figure 2: Comparing theoretical bounds on membership advantage ($\delta = 0$). Improved bound uses Theorem 3.1 to get maximum advantage across all $0 < \alpha \leq 1$.

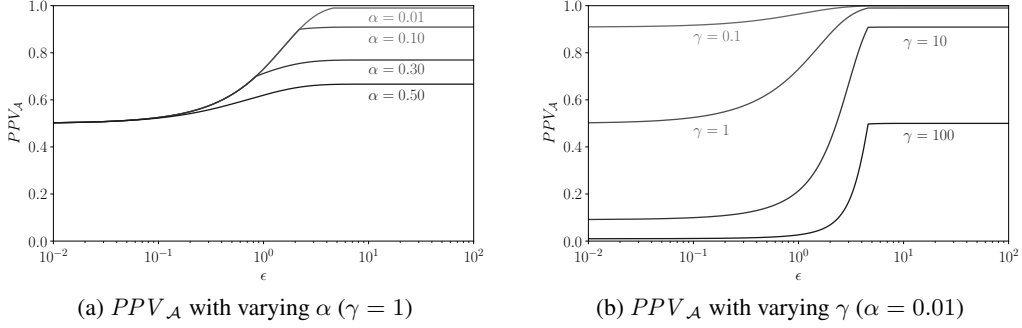


Figure 3: Theoretical upper bounds on PPV metric for various privacy budgets ($\delta = 10^{-5}$).

3.2 Positive Predictive Value

Positive predictive value (PPV) gives the ratio of true members predicted among all the positive membership predictions made by an adversary (the precision of the membership adversary). For an (ϵ, δ) -differentially private algorithm, the PPV is bounded by the following theorem:

Theorem 3.2. Let \mathcal{M} be an (ϵ, δ) -differentially private algorithm and \mathcal{A} be a membership inference adversary. For any randomly chosen record \mathbf{z} and a fixed false positive rate of α , the positive predictive value of \mathcal{A} is bounded by

$$PPV_{\mathcal{A}}(\alpha, \gamma) \leq \frac{1 - f_{\epsilon, \delta}(\alpha)}{1 - f_{\epsilon, \delta}(\alpha) + \gamma\alpha},$$

where $f_{\epsilon, \delta}(\alpha) = \max\{0, 1 - \delta - e^{\epsilon}\alpha, e^{-\epsilon}(1 - \delta - \alpha)\}$, $\gamma = (1 - p)/p$, and p is the prior membership probability defined in Membership Experiment 3.1.

Proof of Theorem 3.2. According to the trade-off function definition (Definition 2.2 and Lemma 2.4), for a given $FPR = \alpha$, we have $1 - TPR \geq f_{\epsilon, \delta}(\alpha)$. Since $PPV_{\mathcal{A}}(\alpha, \gamma) = TP/(TP + FP)$, we can obtain:

$$PPV_{\mathcal{A}}(\alpha, \gamma) = \frac{TPR}{TPR + \gamma \cdot FPR} \leq \frac{1 - f_{\epsilon, \delta}(\alpha)}{1 - f_{\epsilon, \delta}(\alpha) + \gamma\alpha}.$$

□

Like membership advantage, the PPV metric is strictly bounded between 0 and 1. Moreover, the bound on PPV metric considers the prior distribution via γ , which gives the ratio of probability of selecting a non-member to a member. This allows the PPV metric to better capture the privacy threat across different settings. Figure 3a shows the effect of varying the false positive rate α and Figure 3b shows the effect of varying the prior distribution probability γ on the PPV metric. For example, for $\epsilon = 5, \delta = 10^{-5}, \alpha = 0.01, \gamma = 100$, the advantage metric can be as high as 0.98, while the PPV

metric is close to 0.5 (i.e., coin toss probability). Thus, in such scenarios, membership advantage grossly overestimates the privacy threat.

4 Inference Attacks

While the previous section covers the metrics to evaluate privacy leakage, here we discuss about the membership inference attack procedures. In Section 4.1, we describe our threshold selection procedure for threshold-based inference attacks. Section 4.2 presents our threshold-based inference attack that perturbs a query record and uses the direction of change in per-instance loss of the record for membership inference.

4.1 Setting the Decision Threshold

The membership inference attacks we consider need to output a Boolean result for each test, converting a real number measure from a test into a Boolean that indicates whether or not a given input is considered a member. The effectiveness of an attack depends critically on the value of this decision threshold.

We propose a simple procedure to select the decision threshold for any threshold-based attack, which allows the adversary to achieve as much privacy leakage as possible while limited to an expected maximum false positive rate:

Procedure 4.1 (Finding Decision Threshold). Given an adversary, \mathcal{A} , that knows information about a target model including the training data distribution \mathcal{D} , training set size n , training procedure, and model architecture, as well as knowing the prior distribution probability p for the suspected membership set, this procedure finds a threshold ϕ that maximizes the privacy leakage of the sampled data points for a given maximum false positive rate α .

1. Sample a training data set $\bar{S} \sim \mathcal{D}^n$ for training a model $\mathcal{M}_{\bar{S}}$.
2. Randomly sample $b \in \{0, 1\}$, such that $b = 1$ with probability p .
3. Sample record $\mathbf{z} \sim \bar{S}$ if $b = 1$, otherwise $\mathbf{z} \sim \mathcal{D} \setminus \bar{S}$.
4. Output the decision threshold, ϕ , that maximizes its true positive rate constrained to a maximum false positive rate of α for the inference attack, $\mathcal{A}(\mathbf{z}, \mathcal{M}_{\bar{S}}, n, \mathcal{D}, \phi)$.

Note that in comparison to Experiment 3.1, the adversary \mathcal{A} takes an additional parameter ϕ here. With this ϕ , the adversary can query the target model \mathcal{M}_S to perform membership inference. Procedure 4.1 works for any threshold-based inference attack where an adversary knows the data distribution and model training process well enough to train its own models similar to the target model.

Application to Yeom’s Attack. The membership inference attack of Yeom et al. [2018] is one such attack that can benefit from using our threshold selection procedure. As originally designed, the attack uses per-instance loss information for membership inference. Given a loss $\ell(\mathbf{z}, \mathcal{M}_S)$ on the query record \mathbf{z} , their approach classifies it as a member if the loss is less than the expected training loss. Using our Procedure 4.1, we can instead use a threshold ϕ for membership inference that corresponds to an expected maximum false positive rate α . In other words, if the per-instance loss $\ell(\mathbf{z}, \mathcal{M}_S) \leq \phi$, then \mathbf{z} is classified as a member of the target model’s training set S , otherwise it is classified as a non-member. We refer to this membership inference adversary as Yeom.

4.2 Merlin

As discussed above, Procedure 4.1 can be used on any threshold-based inference attack. Here, we introduce a new threshold-based membership inference attack called Merlin¹ that uses a different approach to infer membership. Instead of the per-instance loss of a record, this method uses the direction of change in per-instance loss of the record when it is perturbed with a small amount of noise. The intuition here is that due to overfitting, the target model’s loss on a training set record will

¹Backronym for MEasuring Relative Loss In Neighborhood.

Algorithm 1: Inference Using Direction of Change in Per-Instance Loss

```
1  $\mathcal{A}(\mathbf{z}, \mathcal{M}_S, n, \mathcal{D}, \phi)$ :  
   Input :  $\mathbf{z}$ : input record,  $\mathcal{M}_S$ : model trained on data set  $S$  of size  $n$ ,  $\mathcal{D}$ : data distribution,  $\phi$ :  
           decision function,  $T$ : number of repeat,  $\sigma$ : standard deviation parameter  
   Output : membership prediction of  $\mathbf{z}$  (0 or 1)  
2  $count \leftarrow 0$  ;  
3 for  $T$  runs do  
4   |  $\xi \sim \mathcal{N}(0, \sigma^2 \mathbf{I})$  ; // Sample Gaussian noise  
5   | if  $\ell(\mathbf{z} + \xi, \mathcal{M}_S) > \ell(\mathbf{z}, \mathcal{M}_S)$  then  
6   |   |  $count \leftarrow count + 1$  ;  
7   | end  
8 end  
9 return  $count \geq \phi$  ; // 1 if 'member'
```

Data set	#Features	#Classes	Train Acc	Test Acc	PPV at $\gamma = 1$	PPV at $\gamma = 10$
Purchase-100X	600	100	1.00	0.71	90.11 ± 3.32	55.92 ± 13.32
Texas-100	6,000	100	1.00	0.53	90.93 ± 9.10	(insufficient data)
RCV1X	2,000	52	1.00	0.84	98.00 ± 2.53	81.23 ± 6.28

Table 2: Summary of data sets and results for non-private models. Maximum PPV achieved by Merlin is reported in percentage (averaged across five runs).

tend to be close to a local minimum, so the loss at perturbed points near the original input will be higher. On the other hand, the loss is equally likely to either increase or decrease for a non-member record.

Algorithm 1 describes the attack procedure. For a query record \mathbf{z} , random Gaussian noise with zero mean and standard deviation σ is added and the change of loss direction is recorded. This step is repeated T times and the *count* is incremented each time the per-instance loss of the perturbed record increases. Though we use Gaussian noise, the algorithm works for other noise distributions as well. We also tried uniform distribution and observed similar results, but with different σ values. Both the parameters T and σ can be pre-tuned on a hold-out set to maximize the attacker’s distinguishing power and fixed for the entire attack process. In our experiments, we find $T = 100$ and $\sigma = 0.01$ work well across all data sets. Finally, the query record \mathbf{z} is classified as a member when $count \geq \phi$, where ϕ is a threshold that could be set by Procedure 4.1.

5 Experimental Setup

This section describes the data sets and models used, along with the training procedure and hyperparameter settings. Table 2 summarizes the data sets used and the performance of non-private model trained over each data set. In the balanced prior setting ($\gamma = 1$), members are identified with high confidence ($> 90\%$ PPV) for all the test data sets. The membership inference decreases drastically in the imbalanced prior case, when $\gamma = 10$. Discussion of the results is deferred to Sections 6 and 7.

Data sets. Prior works on both black-box [Shokri et al., 2017, Yeom et al., 2018] and white-box [Nasr et al., 2019] membership inference attacks have shown that multi-class classification tasks are more vulnerable to membership inference. Hence, we select three multi-class classification tasks. Although the three data sets we analyze are public, they are representative of data sets that contain potentially sensitive information about individuals.

– Purchase-100X: Shokri et al. [2017] created Purchase-100 data set by extracting customer transactions from Kaggle’s acquire valued customers challenge Competition [2014]. The authors *arbitrarily* selected 600 items from the transactions data and considered only those customers who purchased

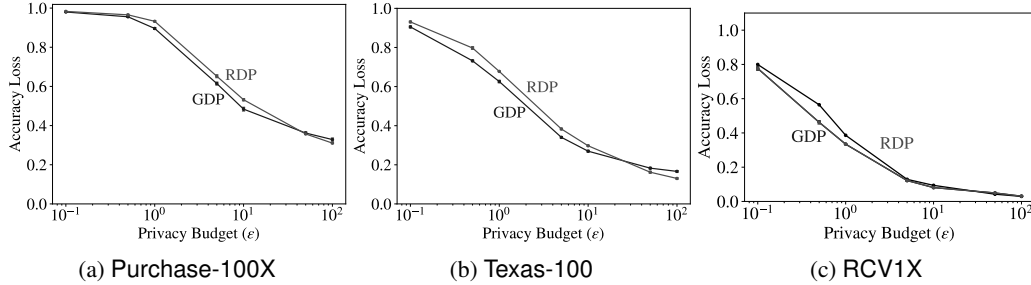


Figure 4: Accuracy loss comparison of private models trained with different privacy analyses.

at least one of the 600 items. Their resulting data set consisted of 197,000 customer records with 600 binary features representing the customer purchase history. Shokri et al. artificially clustered these records into 100 classes, each representing a unique purchase style, such that the goal is to predict a customer’s purchase style. Since we needed more records for our experiments with the $\gamma = 10$ setting, we curated our own data set by following the same procedure. We took the 600 *most frequently* purchased items and ended up with around 300,000 customer records. We call this expanded dataset the Purchase-100X data set.

– Texas-100: We use the Texas hospital data set used by Shokri et al. [2017]. It consists of 67,000 patient records with 6,000 binary features where each feature represents a patient’s medical attribute. This data set also has a 100 output classes where the task is to identify the main procedure that was performed on the patient. This data set is too small for tests with high γ settings, but a useful benchmark for the other settings.

– RCV1X: The Reuters RCV1 corpus dataset [Lewis et al., 2004] is a collection of Reuters newswire articles with more than 800,000 documents, a 47,0000-word vocabulary and 103 classes. The original 103 classes are arranged in a hierarchical manner, and each article can belong to more than one class. We follow data preprocessing procedures similar to Srivastava et al. [2014] to obtain a dataset such that each article only belongs to a single class. The final dataset we use has 420,000 articles, 2,000 most frequent words represented by their term frequencyinverse document frequency (TFIDF) which are used as features and 52 classes. We call our expanded dataset RCV1X.

All the above data sets are pre-processed such that the ℓ_2 norm of each record is bounded by 1. This is a standard pre-processing procedure that improves model performance that is used by many prior works [Chaudhuri et al., 2011, Jayaraman et al., 2018].

Model architecture. We train neural networks with two hidden layers with ReLU activation. Each hidden layer has 256 neurons and the output layer is a softmax layer. Similar multi-layer ReLU network architectures have been used to analyze privacy-preserving deep learning methods in several previous works [Shokri and Shmatikov, 2015, Abadi et al., 2016, Shokri et al., 2017]. Table 2 reports the training and test accuracy of non-private models across the three data sets. As with all of the experimental results we report in this paper, the results are averaged over five runs such that the target model is trained from the scratch for each run. The non-private models for all three data sets achieve 100% training accuracy, but there is a considerable gap between the training and test accuracy. This generalization gap indicates that the model is overfitting the training data, and hence, there is information in the model that could be exploited in a membership inference attack.

Hyperparameters. For each data set, the training set is fixed to 10,000 randomly sampled records and the test set size is varied to reflect different prior probability distributions. For uniform prior ($p = 0.5, \gamma = 1$), we sample 10,000 random records from the remaining data set. For the case of non-uniform prior, we sample γ times the number of training set records to create the test data set. We are most interested in the case where $\gamma > 1$, as it more closely reflects the reality. For both Purchase-100X and RCV1X data sets, we use $\gamma = 2$ ($p \approx 0.333$) and $\gamma = 10$ ($p \approx 0.091$). For Texas-100, we only use $\gamma = 2$ since it is too small for experiments with larger γ .

For training the models, we use the Adam optimizer and perform grid search to find the best values for hyperparameters such as batch size, learning rate, ℓ_2 penalty, clipping threshold and number of

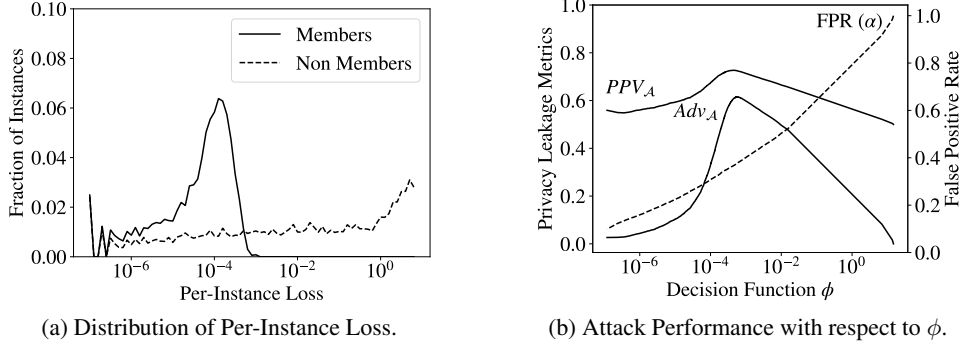


Figure 5: Analysis of Yeom on non-private model trained on Purchase-100X with balanced prior. The x-axis shows the per-instance loss on a logarithmic scale from 10^{-7} to 10^1 where the buckets are in the range $(10^{-7}, 10^{-6.9})$, $(10^{-6.9}, 10^{-6.8})$, and so on up to $(10^{0.9}, 10^1)$.

iterations. We find batch size of 200 and ℓ_2 penalty of 10^{-8} to work the best across all the data sets. For Purchase-100X and Texas-100, we use learning rate of 0.005 and gradient clipping threshold of 4; for RCV1X, we use 0.003 learning rate and 1 gradient clipping threshold. We set the training epochs to 100 for Purchase-100X, 30 for Texas-100, and 80 for RCV1X. We fix the differential privacy failure parameter δ as 10^{-5} to keep it smaller than the inverse of the training set size, generally considered the maximum acceptable value for δ . For an in-depth analysis of hyperparameter tuning on private learning, see Abadi et al. [2016].

Attacks. To study privacy leakage, we perform the two threshold-based membership inference attacks described in Section 4. The first attack, which we refer to as Yeom, uses a threshold on per-instance loss of a given record [Yeom et al., 2018]. The second attack, Merlin, is our proposed approach that uses a threshold on loss direction (see Algorithm 1). The Merlin attack requires tuning the number of repetitions T and noise magnitude σ used in Algorithm 1. Higher values of T usually leads to better membership distinguishability, up to a certain level, but at the cost of computational overhead. We find $T = 100$ to work reasonably well. Merlin’s performance is quite sensitive to σ values. We vary σ between 0.001 and 1 and find $\sigma = 0.01$ to be optimal for Gaussian distribution.

Private Model Training. We evaluate the model accuracy of private neural network models trained on different data sets. We vary the privacy loss budget ϵ between 0.1 and 100 for differential private training and repeat the experiments five times for all the settings to report the average results.

We report the *accuracy loss* metric which gives the relative loss in test accuracy of private models with respect to non-private baseline. The formula for calculating this metric is:

$$Accuracy\ Loss = 1 - \frac{Accuracy\ of\ Private\ Model}{Accuracy\ of\ Non-Private\ Model}$$

Figure 4 gives the accuracy loss of differentially private models trained on different data sets with varying privacy loss budgets. The private models are trained using the gradient perturbation mechanism where the gradients at each epoch are clipped and Gaussian noise is added to preserve privacy. The privacy accounting for composition of mechanisms is done via both Gaussian differential privacy [Dong et al., 2019] (GDP) and the prior state-of-the-art Rényi differential privacy [Mironov, 2017] (RDP). As shown in the figure, the GDP mechanism has a lower accuracy loss for $\epsilon \leq 10$ due to its tighter privacy analysis. The GDP composition theorem requires that the individual mechanisms be highly private, and hence it is hard to reduce noise for $\epsilon > 10$ without increasing the failure probability δ . For all three data sets, GDP performs better than RDP on an average and hence we only report the results for GDP in the remaining experiments.

		α (%)	ϕ	Adv_A (%)	PPV_A (%)
Yeom	Fixed FPR	1.00	-	-	-
	Min FPR	10.00	0	2.13 ± 0.18	54.72 ± 0.44
	Fixed ϕ	-	$(1.04 \pm 0.07) \times 10^{-4}$	35.18 ± 0.69	68.69 ± 0.33
	Max PPV_A	36.00	$(4.12 \pm 0.25) \times 10^{-4}$	61.03 ± 0.50	73.30 ± 0.12
	Max Adv_A	38.00	$(6.49 \pm 0.28) \times 10^{-4}$	62.17 ± 0.22	72.84 ± 0.08
Yeom CBT	Min FPR	0.01	(0, 0, 0)	0.21 ± 0.14	71.30 ± 5.45
	Fixed FPR	1.00	(0, 0, 0)	0.21 ± 0.14	71.30 ± 5.45
	Fixed ϕ	-	$(0.21, 0.82, 1.63) \times 10^{-4}$	33.19 ± 2.06	67.72 ± 0.70
	Max PPV_A	52.00	$(0.79, 4.58, 12.84) \times 10^{-4}$	61.48 ± 0.32	73.07 ± 0.30
	Max Adv_A	57.00	$(0.97, 4.91, 15.38) \times 10^{-4}$	61.80 ± 0.29	73.04 ± 0.29
Merlin	Min FPR	0.01	$(87.60 \pm 1.20)/100$	0.12 ± 0.07	87.02 ± 9.59
	Max PPV_A	0.10	$(84.40 \pm 0.49)/100$	0.46 ± 0.09	90.11 ± 3.32
	Fixed FPR	1.00	$(78.20 \pm 0.40)/100$	2.75 ± 0.22	82.27 ± 0.84
	Max Adv_A	30.00	$(60.40 \pm 0.49)/100$	20.33 ± 0.66	63.13 ± 0.80

Table 3: Thresholds selected against non-private models trained on Purchase-100X with balanced prior. The results are averaged over five runs such that the target model is trained from the scratch for each run. Yeom CBT uses class-based thresholds, where ϕ shows the triplet of minimum, median and maximum thresholds across all classes.

		Texas-100			RCV1X		
		α (%)	Adv_A (%)	PPV_A (%)	α (%)	Adv_A (%)	PPV_A (%)
Yeom	Fixed FPR	1.00	-	-	1.00	-	-
	Min FPR	5.00	2.33 ± 0.22	60.13 ± 0.94	41.00	6.15 ± 3.19	53.27 ± 1.28
	Fixed ϕ	-	52.66 ± 4.56	75.85 ± 1.15	-	27.45 ± 2.21	58.22 ± 0.56
	Max PPV_A	26.00	62.22 ± 5.49	77.15 ± 1.04	67.00	26.57 ± 3.96	58.14 ± 0.85
	Max Adv_A	30.00	66.81 ± 3.60	76.38 ± 0.63	69.00	26.81 ± 3.29	58.08 ± 0.68
Merlin	Min FPR	0.03	0.21 ± 0.22	90.93 ± 9.10	0.01	0.22 ± 0.13	98.00 ± 2.53
	Max PPV_A	0.03	0.21 ± 0.22	90.93 ± 9.10	0.01	0.22 ± 0.13	98.00 ± 2.53
	Fixed FPR	1.00	6.10 ± 1.13	88.08 ± 2.88	1.00	2.74 ± 1.09	79.95 ± 1.75
	Max Adv_A	36.00	38.69 ± 1.23	67.59 ± 0.48	25.00	11.95 ± 1.33	60.20 ± 0.81

Table 4: Comparing membership inference attacks on non-private models across Texas-100 and RCV1X for balanced prior.

6 Threshold Selection

In this section, we evaluate our threshold selection procedure (Procedure 4.1) for both inference attacks. We first consider the Yeom attack, and show that our threshold selection procedure can be used to obtain thresholds that achieve particular attacker goals, such as maximizing the PPV or membership advantage metric, or minimizing the false positive rate. Next, we evaluate the Merlin attack using the same threshold selection procedure and show that it achieves higher PPV metric compared to Yeom. Finally we evaluate the effectiveness of these attacks on differentially private models. For this section, we only consider a balanced prior distribution, as was done in previous work. We defer the results for scenarios with imbalanced priors to Section 7.

6.1 Yeom Attack

The Yeom attack uses a fixed threshold on per-instance loss for membership inference test, such that the query record is classified as a member if its per-instance loss is less than the threshold. We show that the adversary can achieve better privacy leakage, specific to particular attack goals, by using our threshold selection procedure to choose a relevant threshold.

Results on Purchase-100X. We begin by showing the distribution of per-instance loss of members and non-members for a non-private model trained on the Purchase-100X data set in Figure 5a. Per-instance losses of member records are concentrated close to zero, and most of the loss values

are less than 0.001. Whereas for non-member records, the loss values are spread across the range. This suggests that a larger fraction of members will be correctly identified by the attacker with high precision (PPV) for loss thresholds less than 0.001, and hence the privacy leakage will be high. Another notable observation is that 1000.40 ± 34.28 non-members have zero loss across five runs, and hence the minimum achievable false positive rate is 10%. This is reflected in Figure 5b which shows the effect of selecting different loss threshold values on the privacy leakage metrics. An attacker can use our threshold selection procedure to choose a loss threshold to meet specific attack goals, such as minimizing the false positive rate (Min FPR), or achieving a fixed false positive rate (Fixed FPR), or maximizing either of the privacy leakage metrics (Max PPV_A and Max Adv_A). Table 3 summarizes these scenarios and compares their thresholds with the threshold selected by the method of Yeom et al. (Fixed ϕ). For Fixed FPR, we consider an attacker with a false positive rate of 1% ($\alpha = 1\%$). The attacker uses Procedure 4.1 to find loss threshold ϕ corresponding to $\alpha = 1\%$, which it uses for membership inference on the target set. However, since the minimum achievable false positive rate for Yeom on Purchase-100X is 10%, this attack fails to find a suitable threshold. For maximizing PPV or membership advantage, the attacker can use the threshold selection procedure with varying α values and choose the threshold ϕ that maximizes the required privacy metric. In comparison, Fixed ϕ uses a fixed threshold of expected training loss which does not necessarily maximize the privacy leakage. As the results in the table demonstrate, the Yeom attack achieves better privacy leakage when thresholds are chosen using our threshold selection procedure.

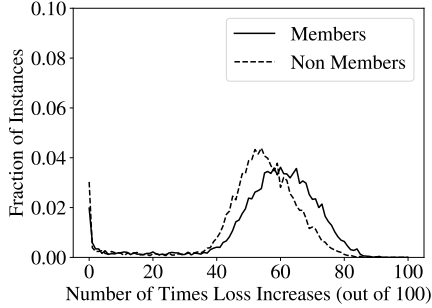
Results on other data sets. While we observe similar trends of privacy leakage corresponding to the selected thresholds for Texas-100 and RCV1X data sets, we discuss the notable differences in the results for these data sets. Table 4 compares the performance of Yeom against non-private models across Texas-100 and RCV1X. We note that Yeom can achieve false positive rates as low as 5% on Texas-100. In general, the attack performance on this data set is comparable to that of Purchase-100X. Appendix A provides more details on the Texas-100 results. For RCV1X, the attack success rate is substantially lower than that for the other data sets (see Table 4). This is because, unlike the other two data sets which have 100 classes, RCV1X is a 52-class classification task. As shown by prior works [Song, 2017, Yeom et al., 2018], success of membership inference attack is proportional to the complexity of classification task. We further note that the maximum PPV that can be achieved by Yeom on RCV1X is only around 58%, at which point the membership advantage is close to 28%. This gives credence to our claim that membership advantage should not be solely relied on as a measure of inference risk. While membership advantage can be high, the privacy leakage is negligible for balanced priors when the PPV is close to 50%. Later in Section 7 we show that this phenomenon is prevalent across all data sets when the prior is imbalanced. Appendix B covers more detailed discussion on the RCV1X results.

Using class-based thresholds. Recently, Song and Mittal [2020] demonstrated that the approach of Yeom et al. [2018] can be further improved by using class-based thresholds instead of one global threshold on loss values. We implement this approach, using our threshold setting algorithm to independently set the threshold for each class (referred as Yeom CBT). This enables finding class-based thresholds corresponding to smaller α values, as seen for the minimum FPR ($\alpha = 0.01$) and fixed FPR ($\alpha = 1$) cases for Purchase-100X in Table 3. Nonetheless, the maximum PPV still does not exceed that of Yeom. We observe similar results for Texas-100 (reported in Appendix A) and RCV1X (Appendix B).

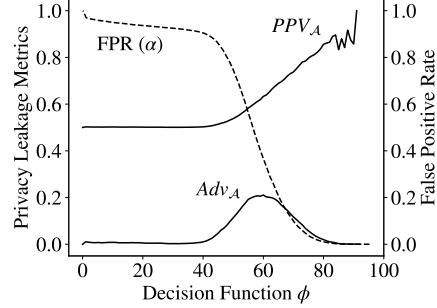
6.2 Merlin Attack

Next, we perform inference attacks using the Merlin (Algorithm 1) where the attacker perturbs a record with random Gaussian noise of magnitude $\sigma = 0.01$ and notes the direction of change in loss. This process is repeated $T = 100$ times and the attacker infers the membership of the record based on the number of times the loss increases out of 100 trials. More concretely, if the loss increases more than a threshold number of times, then the record is classified as a member. As with the Yeom experiments, we use Procedure 4.1 to select a suitable threshold.

Results on Purchase-100X. Figure 6a shows the distribution of loss direction counts for member and non-member records for a non-private model trained on the Purchase-100X data set. The loss increases 56.77 ± 16.74 times out of 100 trials on an average for member records, whereas for the



(a) Distribution of Increase in Loss Count.



(b) Attack Performance with respect to ϕ .

Figure 6: Analysis of Merlin on non-private model trained on Purchase-100X with balanced prior.

ϵ	α (%)	Yeom		Merlin		
		ϕ	Max PPV_A (%)	α (%)	ϕ (out of 100)	Max PPV_A (%)
1	4.00	0.45 ± 0.04	57.27 ± 1.37	2.00	78.20 ± 0.40	53.57 ± 1.26
10	15.00	$(8.50 \pm 0.80) \times 10^{-3}$	60.47 ± 0.51	2.00	77.60 ± 0.49	59.10 ± 1.64
100	27.00	$(1.48 \pm 0.12) \times 10^{-3}$	61.10 ± 0.33	0.30	82.60 ± 0.49	63.82 ± 4.62

Table 5: Membership inference attacks against private models trained on Purchase-100X data set with balanced prior.

non-member records the loss increases 51.84 ± 15.58 times on an average. Thus, the attacker can identify more member records with high precision when it chooses a threshold greater than 56. A peculiar observation is that the loss direction count is zero for a considerable fraction of members and non-members. For the non-member records, the loss is very high to begin with and hence it always decreases on adding noise. Whereas for the member records with zero count, the loss value does not change even with addition of noise. As mentioned in step 5 of Algorithm 1, we only check if the loss increases upon perturbation since we believe that equality is not a strong indicator of membership. Figure 6b shows the attack performance with varying thresholds. As shown, Merlin can achieve much higher PPV than Yeom. Table 3 summarizes the thresholds selected by Merlin with different attack goals and compares the performance with Yeom. While Yeom can only achieve a minimum false positive rate of 10% on this data set, Merlin can achieve false positive rate as low as 0.01%. Thus Merlin is successful at a fixed false positive rate of 1% where Yeom fails. Another notable observation is that Merlin can achieve close to 90% PPV while the maximum possible PPV achievable via Yeom is around 73%. Thus, this attack is more suitable for scenarios where attack precision is preferred.

Results on other data sets. Table 4 compares the membership inference attack performance against non-private models across Texas-100 and RCV1X. The Merlin attack allows for thresholds corresponding to smaller false positive rates and consistently achieves higher PPV than Yeom across all the data sets. Merlin is more successful on Texas-100 compared to Purchase-100X, as the gap between loss direction distribution of member records and non-member records is high for Texas-100 (see Appendix A for more analysis). More surprisingly, while Yeom is less successful on RCV1X, we find that Merlin still manages to achieve a very high PPV (See Table 4). Thus, Merlin poses privacy threat even in scenarios where Yeom fails. Appendix B provides details on the RCV1X results.

Using class-based thresholds. We also tried class-based thresholds for Merlin, like we did for Yeom. However, we found that this approach does not benefit Merlin as the individual classes do not have significant number of records to provide meaningful thresholds. By using class based threshold, the maximum achievable PPV for Merlin reduced from around 90.11% to 84.55%, meanwhile the advantage metric increased from 0.46% to 2.99%. We observed similar behaviour across different thresholds.

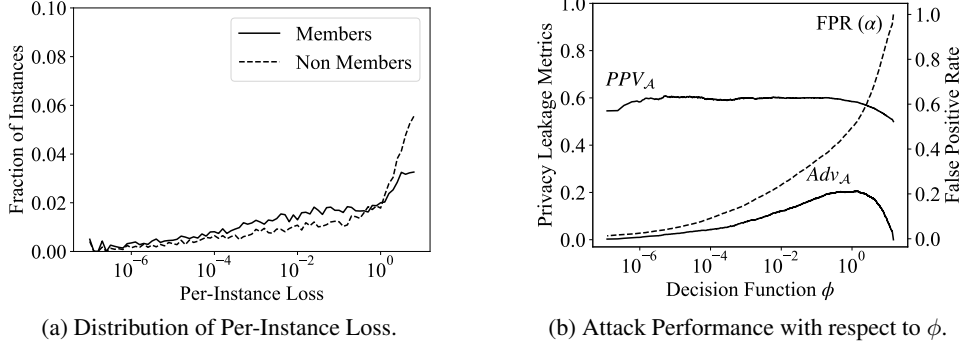


Figure 7: Analysis of Yeom on private model trained with $\epsilon = 100$ at $\gamma = 1$ (Purchase-100X).

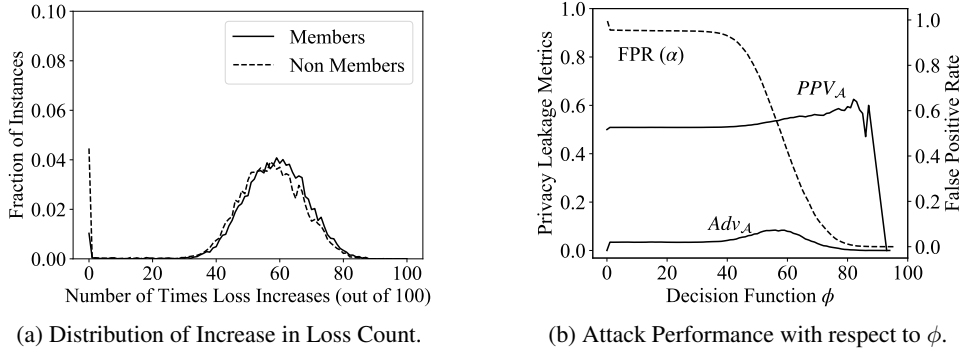


Figure 8: Analysis of Merlin on private model trained with $\epsilon = 100$ at $\gamma = 1$ (Purchase-100X).

6.3 Impact of Privacy Noise

We also evaluated membership inference attacks against the private models and found no threshold that appears to pose a serious privacy threat against these models. Similar to the experiments with non-private models, here also we repeat the experiments five times and report the averaged results. In each run, we train the private model from the scratch and perform the attack procedure on it. Table 5 compares the maximum PPV achieved by Yeom and Merlin attacks against private models trained on Purchase-100X with varying privacy loss budgets. As expected, the privacy leakage increases with increasing privacy loss budget. However the privacy threat is not significant as the PPV is close to 60% even for $\epsilon = 100$, a privacy loss budget large enough to provide no meaningful theoretical privacy guarantee.

To understand how the privacy noise is impacting the attack success, we plot the loss distribution of member and non-member records for a private model trained with $\epsilon = 100$ in Figure 7a. The figure shows that the noise reduces the gap between the two distributions when compared to Figure 5a with no privacy. Hence differential privacy limits the success of Yeom by spreading out the loss values for both member and non-member distributions. Though in doing so, it also reduces the number of non-member records with zero loss from 1000.40 ± 34.28 (in non-private case) to 121.60 ± 22.02 . This reduces the minimum achievable false positive rate to 0.01%, and hence allows the attacker to set α thresholds smaller than 10% against private models which wasn't possible in the non-private case. However the PPV is still less than 60% for these thresholds. Figure 7b shows the attack performance at different thresholds. Due to the reduced gap between the member and non-member loss distributions, the PPV is close to 60% across all loss thresholds even if the maximum membership advantage is considerable (close to 20% for $\epsilon = 100$). Thus even with small privacy noise, the privacy leakage risk is significantly mitigated. We observe similar trends across the other two data sets and hence defer these results to Appendix A and B.

Next, we plot the performance of Merlin on a private model trained with $\epsilon = 100$. Figure 8a shows the distribution of loss direction counts for member and non-member records. When compared to the corresponding distribution for a non-private model (see Figure 6a), the gap between the distributions

γ	Max PPV_A of Yeom (%)			Max PPV_A of Merlin (%)		
	Purchase-100X	Texas-100	RCV1X	Purchase-100X	Texas-100	RCV1X
1	73.30 \pm 0.12	77.15 \pm 1.04	58.14 \pm 0.85	90.11 \pm 3.32	90.93 \pm 9.10	98.00 \pm 2.53
2	57.86 \pm 0.38	61.52 \pm 1.85	42.02 \pm 0.44	84.91 \pm 13.88	83.38 \pm 8.70	97.10 \pm 1.83
10	21.25 \pm 0.28	-	12.59 \pm 0.36	55.92 \pm 13.32	-	81.23 \pm 6.28

Table 6: Effect of varying γ on PPV metric against non-private models.

is greatly reduced. This restricts the privacy leakage across all thresholds, as shown in Figure 8b. We note that the PPV in the figure goes to zero for the threshold corresponding to the minimum false positive rate. This is because PPV drastically fluctuates between 0 and 1 across all five runs for minimum FPR, and we do not cherry pick a run to report. The PPV is 1 for two out of five runs and 0 for the other runs. We observe similar trends for Merlin on the other two data sets, and hence defer their results to the appendices. In conclusion, none of the attacks pose a meaningful privacy threat against differentially private models, even when the privacy loss budget is as large as $\epsilon = 100$.

7 Imbalanced Scenarios

As discussed in Section 3, the membership advantage metric does not capture the prior distribution probability and hence gives a false sense of privacy threat for imbalanced prior settings where $\gamma > 1$. In this section, we provide empirical evidence that the PPV metric captures privacy leakage more naturally in imbalanced prior settings, and hence is a more reliable metric for evaluating the privacy leakage.

In the imbalanced prior setting, the pool from which the attacker samples records for inference testing has γ times more non-member records than members. In other words, the attacker is γ times more likely to randomly pick a non-member than a member record for testing. For this experimental setting, we set γ as high as the data set allows, such that the training set is fixed to 10,000 records as in the previous experiments but the test set size is γ times the training set size. As discussed in Section 5, we constructed expanded versions of the Purchase-100 and RCV1 datasets to enable these experiments. Both the Purchase-100X and RCV1X data sets have more than 200,000 records, and hence are large enough to allow setting $\gamma = 10$. We did not have source data to expand Texas-100, so are left with a data set with only 67,000 records and hence only have results for $\gamma = 2$. The threshold selection procedure (Procedure 4.1) uses holdout training and test sets that are disjoint from the target training and test sets mentioned above, so the data set has to have at least $(\gamma + 1) \times 20,000$ records to run the experiments.

Table 6 shows the effect of varying γ on the maximum PPV of membership inference attacks against non-private models trained on different data sets. We can see a clear drop in PPV values across all data sets with increasing γ values. The maximum PPV drops by around 10 - 15% on an average between $\gamma = 1$ and $\gamma = 2$. For $\gamma = 2$, the maximum PPV of Yeom is close to 60%, whereas Merlin still achieves a comparatively higher PPV of around 84%. Hence, Merlin still poses some privacy threat at $\gamma = 2$. However, as the γ value increases to 10, none of the attacks are successful. Though we note that Merlin is still somewhat successful on RCV1X at $\gamma = 10$. On the other hand, the membership advantage values remain more or less the same across different γ values for both Yeom and Merlin on Purchase-100X, as shown in Figure 9. We observe the same trend for Texas-100 and RCV1X. Plots for these data sets are found in the appendix (Figures 14 and 19). These results support our claim that PPV is a more reliable metric in imbalanced prior scenarios.

None of the attacks pose a privacy threat in the imbalanced prior settings where γ values are higher than 10. In many practical scenarios, we would expect the γ to be much higher, in which case the membership inference attacks would be even less likely to succeed. Balanced priors is the best case scenario for a membership inference adversary to show high privacy leakage, but also a setting where the actual risk of being identified as a member is likely to be low since half the population under consideration are expected to be members. Since the private models are not vulnerable to inference attacks in the balanced prior setting, we conclude that they will not be vulnerable in the imbalanced

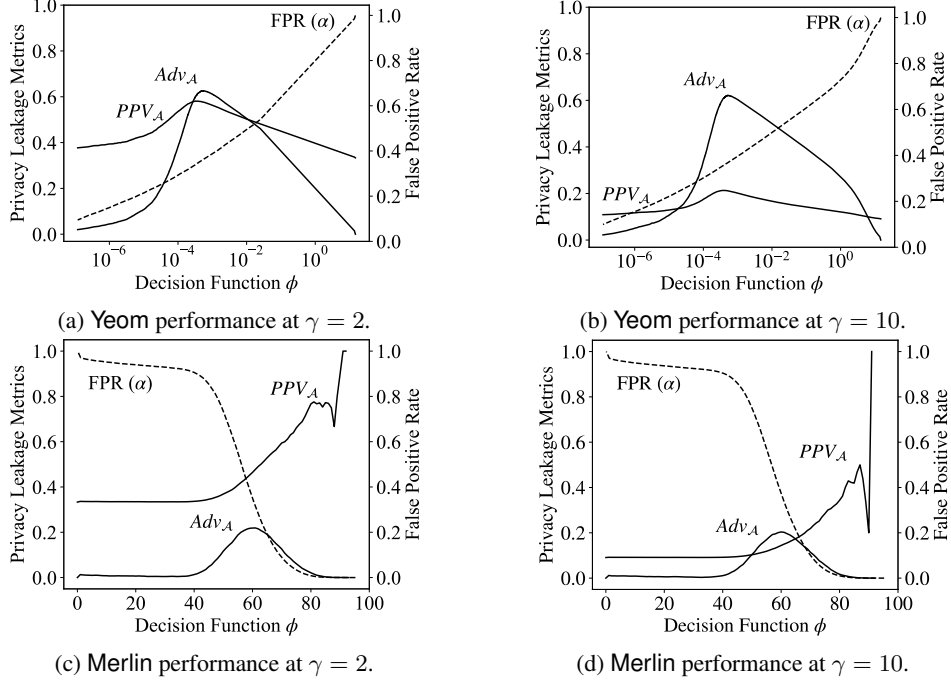


Figure 9: Attack performance on Purchase-100X for imbalanced prior setting.

prior setting as well, where $\gamma > 1$. Hence we do not show the membership inference attack results against private models.

8 Conclusion

Understanding privacy risks for machine learning poses considerable challenges, and there remains a large gap between what can be guaranteed and the effectiveness of attacks in practice. In this work, we introduce a novel threshold selection procedure that allows adversaries to choose inference thresholds specific to their attack goals, and demonstrate a new membership inference attack, Merlin, that outperforms previous attacks in the settings that matter the most. From experiments on three real world data sets under different prior distribution settings, we find that although the non-private models are highly vulnerable in the balanced prior setting, even a small amount of privacy noise mitigates the privacy risk. Even with the improved attack, however, our results show no evidence of privacy risk in imbalanced prior scenarios, even when no privacy mechanisms are used.

While membership inference has been shown to be a serious threat in balanced prior settings, our results show that this is not the case under more realistic assumptions where only a small fraction of the candidate population is included in the training data. These results raise doubts about the practicality of membership inference attacks for most settings, but do not mean that other privacy threats are not present. For instance, attribute inference attacks are more prominent privacy threats, where skewed priors for sensitive attribute values are not uncommon. Moreover, our results show that there is negligible membership inference risk on average, but do not dismiss the possibility that certain subpopulation could be at risk. We hope our work encourages further research into understanding more realistic settings for inference attacks, and developing meaningful privacy-utility trade-offs for these scenarios.

Availability

All of our code and data for our experiments is available at <https://github.com/bargavj/EvaluatingDPML>.

Acknowledgments

This work was partially supported by grants from the National Science Foundation (#1717950 and #1915813).

References

- Martin Abadi, Andy Chu, Ian Goodfellow, H. Brendan McMahan, Ilya Mironov, Kunal Talwar, and Li Zhang. Deep learning with differential privacy. In *ACM Conference on Computer and Communications Security*, 2016.
- Galen Andrew, Steve Chien, and Nicolas Papernot. TensorFlow Privacy. <https://github.com/tensorflow/privacy>, 2019.
- Giuseppe Ateniese, Luigi Mancini, Angelo Spognardi, Antonio Villani, Domenico Vitali, and Giovanni Felici. Hacking smart machines with smarter ones: How to extract meaningful data from machine learning classifiers. *International Journal of Security and Networks*, 2015.
- Borja Balle and Yu-Xiang Wang. Improving the gaussian mechanism for differential privacy: Analytical calibration and optimal denoising. In *International Conference on Machine Learning*, 2018.
- Borja Balle, Gilles Barthe, Marco Gaboardi, Justin Hsu, and Tetsuya Sato. Hypothesis testing interpretations and renyi differential privacy. *arXiv:1905.09982*, 2019.
- Brett K Beaulieu-Jones, William Yuan, Samuel G Finlayson, and Zhiwei Steven Wu. Privacy-preserving distributed deep learning for clinical data. *arXiv:1812.01484*, 2018.
- Abhishek Bhowmick, John Duchi, Julien Freudiger, Gaurav Kapoor, and Ryan Rogers. Protection against reconstruction and its applications in private federated learning. *arXiv:1812.00984*, 2018.
- Zhiqi Bu, Jinshuo Dong, Qi Long, and Weijie J Su. Deep learning with gaussian differential privacy. *arXiv:1911.11607*, 2019.
- Mark Bun and Thomas Steinke. Concentrated differential privacy: Simplifications, extensions, and lower bounds. In *Theory of Cryptography Conference*, 2016.
- Kamalika Chaudhuri, Claire Monteleoni, and Anand D. Sarwate. Differentially private empirical risk minimization. *Journal of Machine Learning Research*, 2011.
- Kaggle Competition. Acquire valued shoppers challenge, 2014. URL <https://kaggle.com/c/acquire-valued-shoppers-challenge/data>.
- Jinshuo Dong, Aaron Roth, and Weijie J Su. Gaussian differential privacy. *arXiv:1905.02383*, 2019.
- Cynthia Dwork and Guy N. Rothblum. Concentrated differential privacy. *arXiv:1603.01887*, 2016.
- Cynthia Dwork, Frank McSherry, Kobbi Nissim, and Adam Smith. Calibrating Noise to Sensitivity in Private Data Analysis. In *Theory of Cryptography Conference*, 2006.
- Farhad Farokhi and Mohamed Ali Kaafar. Modelling and quantifying membership information leakage in machine learning. *arXiv:2001.10648*, 2020.
- Matt Fredrikson, Somesh Jha, and Thomas Ristenpart. Model inversion attacks that exploit confidence information and basic countermeasures. In *ACM Conference on Computer and Communications Security*, 2015.
- Matthew Fredrikson, Eric Lantz, Somesh Jha, Simon Lin, David Page, and Thomas Ristenpart. Privacy in Pharmacogenetics: An end-to-end case study of personalized Warfarin dosing. In *USENIX Security Symposium*, 2014.
- Karan Ganju, Qi Wang, Wei Yang, Carl A Gunter, and Nikita Borisov. Property inference attacks on fully connected neural networks using permutation invariant representations. In *ACM Conference on Computer and Communications Security*, 2018.

- Robin C Geyer, Tassilo Klein, and Moin Nabi. Differentially private federated learning: A client level perspective. *arXiv:1712.07557*, 2017.
- Nick Hynes, Raymond Cheng, and Dawn Song. Efficient deep learning on multi-source private data. *arXiv:1807.06689*, 2018.
- Prateek Jain and Abhradeep Thakurta. Differentially private learning with kernels. In *International Conference on Machine Learning*, 2013.
- Bargav Jayaraman and David Evans. Evaluating differentially private machine learning in practice. In *USENIX Security Symposium*, 2019.
- Bargav Jayaraman, Lingxiao Wang, David Evans, and Quanquan Gu. Distributed learning without distress: Privacy-preserving empirical risk minimization. In *Advances in Neural Information Processing Systems*, 2018.
- Peter Kairouz, Sewoong Oh, and Pramod Viswanath. The composition theorem for differential privacy. *IEEE Transactions on Information Theory*, 2017.
- David D Lewis, Yiming Yang, Tony G Rose, and Fan Li. RCV1: A new benchmark collection for text categorization research. *Journal of Machine Learning Research*, 2004.
- Changchang Liu, Xi He, Thee Chanyaswad, Shiqiang Wang, and Prateek Mittal. Investigating statistical privacy frameworks from the perspective of hypothesis testing. *Proceedings on Privacy Enhancing Technologies*, 2019.
- Yunhui Long, Vincent Bindschaedler, and Carl A. Gunter. Towards measuring membership privacy. *arXiv:1712.09136*, 2017.
- Daniel Lowd and Christopher Meek. Adversarial learning. In *ACM SIGKDD International Conference on Knowledge Discovery and Data Mining*, 2005.
- Ilya Mironov. Rényi differential privacy. In *IEEE Computer Security Foundations Symposium*, 2017.
- Milad Nasr, Reza Shokri, and Amir Houmansadr. Comprehensive privacy analysis of deep learning. In *IEEE Symposium on Security and Privacy*, 2019.
- Md Atiqur Rahman, Tanzila Rahman, Robert Laganiere, Noman Mohammed, and Yang Wang. Membership inference attack against differentially private deep learning model. *Transactions on Data Privacy*, 2018.
- Ahmed Salem, Yang Zhang, Mathias Humbert, Pascal Berrang, Mario Fritz, and Michael Backes. ML-Leaks: Model and data independent membership inference attacks and defenses on machine learning models. In *Network and Distributed Systems Security Symposium*, 2019.
- Reza Shokri and Vitaly Shmatikov. Privacy-preserving deep learning. In *ACM Conference on Computer and Communications Security*, 2015.
- Reza Shokri, Marco Stronati, Congzheng Song, and Vitaly Shmatikov. Membership inference attacks against machine learning models. In *IEEE Symposium on Security and Privacy*, 2017.
- Congzheng Song. Code for membership inference attack against machine learning models. <https://github.com/csong27/membership-inference>, 2017.
- Liwei Song and Prateek Mittal. Systematic evaluation of privacy risks of machine learning models. *arXiv:2003.10595*, 2020.
- Nitish Srivastava, Geoffrey Hinton, Alex Krizhevsky, Ilya Sutskever, and Ruslan Salakhutdinov. Dropout: A simple way to prevent neural networks from overfitting. *Journal of Machine Learning Research*, 2014.
- Florian Tramèr, Fan Zhang, Ari Juels, Michael K Reiter, and Thomas Ristenpart. Stealing machine learning models via prediction APIs. In *USENIX Security Symposium*, 2016.

- Binghui Wang and Neil Zhenqiang Gong. Stealing hyperparameters in machine learning. In *IEEE Symposium on Security and Privacy*, 2018.
- Larry Wasserman and Shuheng Zhou. A statistical framework for differential privacy. *Journal of the American Statistical Association*, 2010.
- Mengjia Yan, Christopher Fletcher, and Josep Torrellas. Cache telepathy: Leveraging shared resource attacks to learn DNN architectures. In *USENIX Security Symposium*, 2020.
- Samuel Yeom, Irene Giacomelli, Matt Fredrikson, and Somesh Jha. Privacy risk in machine learning: Analyzing the connection to overfitting. In *IEEE Computer Security Foundations Symposium*, 2018.
- Jun Zhang, Zhenjie Zhang, Xiaokui Xiao, Yin Yang, and Marianne Winslett. Functional mechanism: Regression analysis under differential privacy. *The VLDB Journal*, 2012.
- Lingchen Zhao, Yan Zhang, Qian Wang, Yanjiao Chen, Cong Wang, and Qin Zou. Privacy-preserving collaborative deep learning with irregular participants. *arXiv:1812.10113*, 2018.

A Results for Texas-100

We recall that Texas-100 is a 100 class classification data set consisting of patient health records where the class label identifies the type of major procedure the patient underwent. Hence the privacy risk is significant for this data set as a successful membership inference would reveal that a particular person was admitted as a patient and underwent a medical procedure.

A.1 Non-private models trained on Texas-100

As with Purchase-100X, we plot the distribution of per-instance loss of member and non-member records for a non-private model trained on Texas-100 data set (see Figure 10a). A notable difference is that the number of non-member records having zero loss is lower than that of Purchase-100X. As a result, the false positive rate can be as low as 5% for this data set. This is depicted in Figure 10b which shows the performance of Yeom against a non-private model at different thresholds. The trend is similar to what we observe for Purchase-100X data set.

Figure 11a shows the distribution of loss direction counts of members and non-members for Merlin against a non-private model trained on Texas-100 data set. The gap between the member and non-member distributions is greater than that of Purchase-100X and hence this attack is more effective on this data set. An important indicator for this is that almost none of the member records have zero count whereas 613.00 ± 36.89 non-member records have zero count. Thus for this data set, the loss of member records almost always increase when perturbed with small noise. On an average the loss increases 80.95 ± 11.68 out of 100 times for member records whereas it increases 64.59 ± 21.69 out of 100 times for non-member records. Figure 11b shows the performance of Merlin on non-private model trained on Texas-100 data set at different count thresholds. Though the threshold values are different, but the trend is similar to what we observed for Purchase-100X data set. These results further validate the effectiveness of selecting a good threshold based on our proposed procedure. Table 7 compares the membership inference attacks across different attack settings on Texas-100. As shown, Merlin achieves much higher PPV values than Yeom. An interesting observation is that using class based thresholds drastically improves PPV values for Yeom. While Yeom CBT achieves higher PPV than Merlin on an average, we note that Merlin has high variance and can achieve up to 100% PPV in some runs. As with Purchase-100X, we observe no benefit of using class based thresholds for Merlin.

		α (%)	ϕ	Adv_A (%)	PPV_A (%)
Yeom	Fixed FPR	1.00	-	-	-
	Min FPR	5.00	0	2.33 ± 0.22	60.13 ± 0.94
	Fixed ϕ	-	$(3.85 \pm 6.67) \times 10^{-3}$	52.66 ± 4.56	75.85 ± 1.15
	Max PPV_A	26.00	$(1.50 \pm 0.05) \times 10^{-3}$	62.22 ± 5.49	77.15 ± 1.04
	Max Adv_A	30.00	$(4.35 \pm 0.25) \times 10^{-3}$	66.81 ± 3.60	76.38 ± 0.63
Yeom CBT	Min FPR	0.03	$(0, 2.57 \times 10^{-6}, 2.38 \times 10^{-2})$	9.26 ± 0.86	93.45 ± 0.36
	Fixed FPR	1.00	$(0, 3.22 \times 10^{-6}, 2.38 \times 10^{-2})$	10.28 ± 1.27	92.58 ± 0.18
	Fixed ϕ	-	$(0.12, 5.1, 30.1) \times 10^{-4}$	48.15 ± 5.02	76.76 ± 1.27
	Max PPV_A	0.03	$(0, 2.57 \times 10^{-6}, 2.38 \times 10^{-2})$	9.26 ± 0.86	93.45 ± 0.36
	Max Adv_A	66.00	$(3.50 \times 10^{-6}, 3.71 \times 10^{-3}, 8.22)$	66.82 ± 3.57	76.76 ± 0.39
Merlin	Min FPR	0.03	$(99.80 \pm 0.40)/100$	0.21 ± 0.22	90.93 ± 9.10
	Max PPV_A	0.03	$(99.80 \pm 0.40)/100$	0.21 ± 0.22	90.93 ± 9.10
	Fixed FPR	1.00	$(95.20 \pm 0.40)/100$	6.10 ± 1.13	88.08 ± 2.88
	Max Adv_A	36.00	$(75.60 \pm 0.49)/100$	38.69 ± 1.23	67.59 ± 0.48

Table 7: Thresholds selected against non-private models trained on Texas-100 with balanced prior. The results are averaged over five runs such that the target model is trained from the scratch for each run. Yeom CBT uses class-based thresholds, where ϕ shows the triplet of minimum, median and maximum thresholds across all classes.

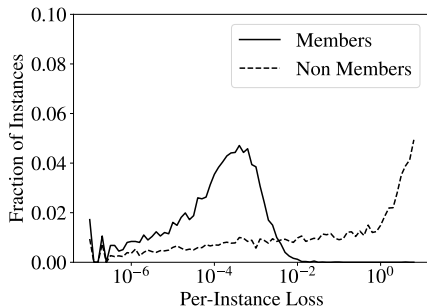
ϵ	α (%)	Yeom		Merlin		
		ϕ	Max PPV_A (%)	α (%)	ϕ (out of 100)	Max PPV_A (%)
1	10.00	1.19 ± 0.02	51.48 ± 0.56	1.00	88.40 ± 0.49	53.93 ± 1.71
10	21.00	$(3.68 \pm 0.31) \times 10^{-1}$	53.80 ± 0.45	6.00	84.40 ± 0.49	56.37 ± 1.46
100	21.00	$(1.25 \pm 0.08) \times 10^{-1}$	54.94 ± 0.19	7.00	85.00 ± 0.00	57.68 ± 0.91

Table 8: Membership inference attacks against private models trained on Texas-100 data set with balanced prior.

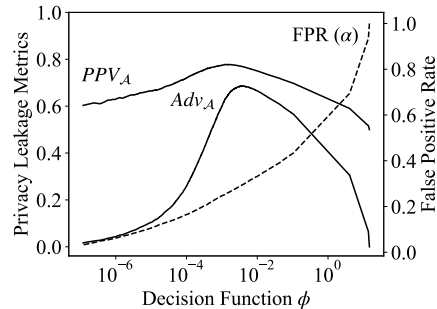
A.2 Private models trained on Texas-100

Table 8 compares the maximum PPV achieved by Yeom and Merlin attacks against private models trained on Texas-100 with varying privacy loss budgets. As expected, the privacy leakage increases with increase in privacy loss budget. However the privacy threat is not significant as the PPV is less than 60% even for a large privacy loss budget $\epsilon = 100$, where there is no theoretical privacy guarantee.

To show how the privacy noise is impacting the attack success, we plot the loss distribution of member and non-member records for a private model trained with $\epsilon = 100$ in Figure 12a. The figure shows that the noise reduces the gap between the two distributions when compared to Figure 10a with no privacy. Hence differential privacy limits the success of Yeom by spreading out the loss values for both member and non-member distributions, as we saw in the case of Purchase-100X. Though in doing so, it also reduces the number of non-member records with zero loss from 339.20 ± 33.47 (in non-private case) to zero. This allows the attacker to set α thresholds smaller than 5% against private

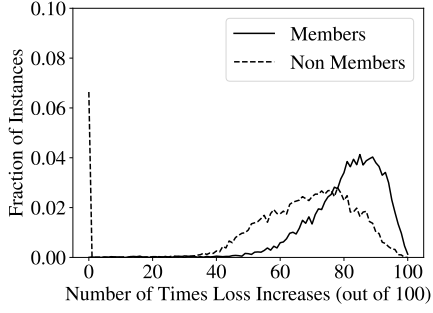


(a) Distribution of Per-Instance Loss.

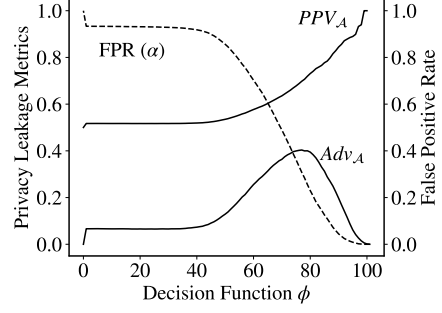


(b) Attack Performance with respect to ϕ .

Figure 10: Analysis of Yeom on non-private model trained on Texas-100 with balanced prior.

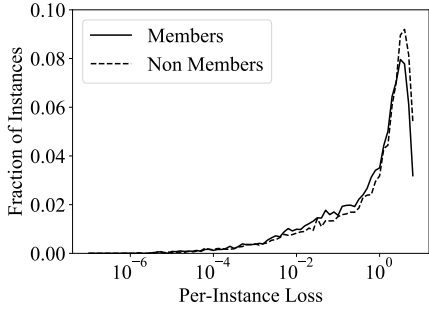


(a) Distribution of Increase in Loss Count.

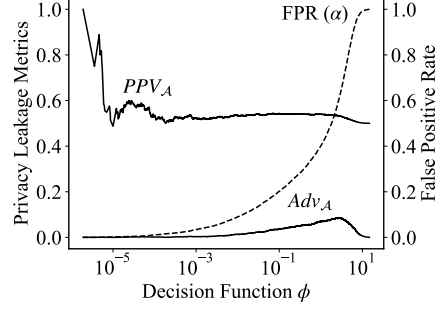


(b) Attack Performance with respect to ϕ .

Figure 11: Analysis of Merlin on non-private model trained on Texas-100 with balanced prior.

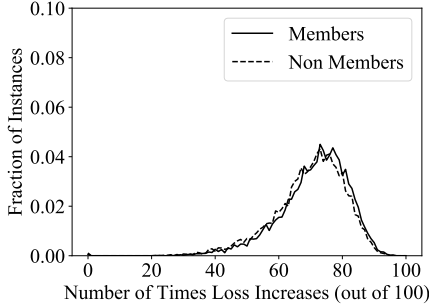


(a) Distribution of Per-Instance Loss.

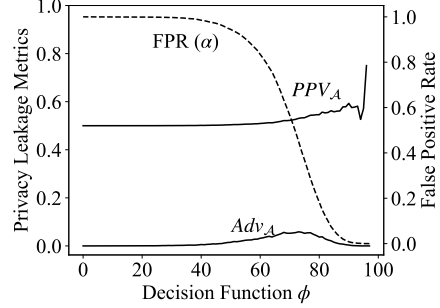


(b) Attack Performance with respect to ϕ .

Figure 12: Analysis of Yeom on private model trained with $\epsilon = 100$ at $\gamma = 1$ (Texas-100).

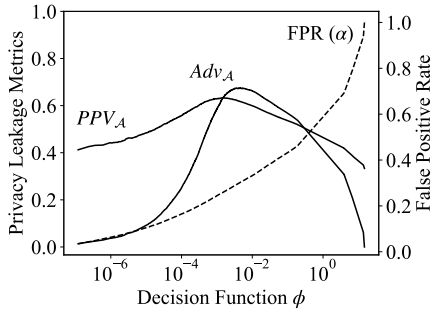


(a) Distribution of Per-Instance Loss.

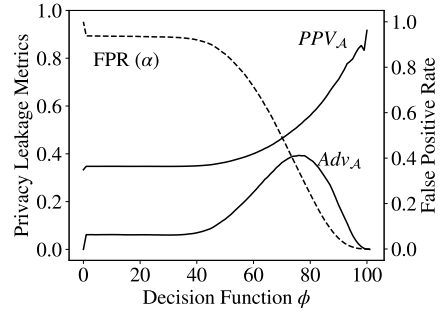


(b) Attack Performance with respect to ϕ .

Figure 13: Analysis of Merlin on private model trained with $\epsilon = 100$ at $\gamma = 1$ (Texas-100).



(a) Yeom performance at $\gamma = 2$.



(b) Merlin performance at $\gamma = 2$.

Figure 14: Attack performance on Texas-100 for imbalanced prior setting.

		α (%)	ϕ	$Adv_{\mathcal{A}}$ (%)	$PPV_{\mathcal{A}}$ (%)
Yeom	Fixed FPR	1.00	-	-	-
	Min FPR	41.00	0	6.15 ± 3.19	53.27 ± 1.28
	Fixed ϕ	-	$(2.15 \pm 1.81) \times 10^{-3}$	27.45 ± 2.21	58.22 ± 0.56
	Max $PPV_{\mathcal{A}}$	67.00	$(1.38 \pm 1.59) \times 10^{-3}$	26.57 ± 3.96	58.14 ± 0.85
	Max $Adv_{\mathcal{A}}$	69.00	$(2.17 \pm 0.24) \times 10^{-3}$	26.81 ± 3.29	58.08 ± 0.68
Yeom CBT	Min FPR	0.01	$(0, 0, 1.72) \times 10^{-4}$	1.68 ± 0.80	93.76 ± 1.40
	Max $PPV_{\mathcal{A}}$	0.01	$(0, 0, 1.72) \times 10^{-4}$	1.68 ± 0.80	93.76 ± 1.40
	Fixed FPR	1.00	$(0, 0, 1.72) \times 10^{-4}$	1.78 ± 0.92	92.81 ± 5.63
	Fixed ϕ	-	$(0.18, 1.60, 92.1) \times 10^{-3}$	20.97 ± 3.30	56.95 ± 0.56
	Max $Adv_{\mathcal{A}}$	71.00	$(0, 8.94 \times 10^{-3}, 7.68)$	24.41 ± 3.70	58.72 ± 1.10
Merlin	Min FPR	0.01	$(97.00 \pm 0.63)/100$	0.22 ± 0.13	98.00 ± 2.53
	Max $PPV_{\mathcal{A}}$	0.01	$(97.00 \pm 0.63)/100$	0.22 ± 0.13	98.00 ± 2.53
	Fixed FPR	1.00	$(87.60 \pm 1.02)/100$	2.74 ± 1.09	79.95 ± 1.75
	Max $Adv_{\mathcal{A}}$	25.00	$(67.20 \pm 0.40)/100$	11.95 ± 1.33	60.20 ± 0.81

Table 9: Thresholds selected against non-private models trained on RCV1X with balanced prior. The results are averaged over five runs such that the target model is trained from the scratch for each run. Yeom CBT uses class-based thresholds, where ϕ shows the triplet of minimum, median and maximum thresholds across all classes.

models which wasn’t possible in the non-private case. However the PPV is still less than 55% for these thresholds. Figure 12b shows the attack performance at different thresholds. While there is high variance at smaller thresholds, on an average the maximum PPV is close to 55%. Thus even with small privacy noise, the privacy leakage risk is significantly mitigated.

Next we plot the performance of Merlin on a private model trained with $\epsilon = 100$ in Figure 13. Figure 13a shows the distribution of loss direction counts for member and non-member records. When compared to the corresponding distribution for a non-private model (see Figure 11a), the gap between the distributions is greatly reduced. This restricts the privacy leakage across all thresholds as shown in Figure 13b.

A.3 Imbalanced prior setting for Texas-100

Since Texas-100 only has 67,000 records, we were only able test for $\gamma = 2$. Figure 14a shows the performance of Yeom across different thresholds. When compared to Figure 10b, we can see a clear drop in PPV values across all thresholds. Though the maximum PPV is still considerable enough to pose privacy risk. In practice, we would observe much higher values of γ where these attacks would fail, as shown for $\gamma = 10$ setting on Purchase-100X. As expected, the membership advantage remains unchanged between balanced and imbalanced prior settings. Figure 14b shows the performance of Merlin on Texas-100 at $\gamma = 2$ setting. We observe the same trend as that of Yeom. The membership advantage values remain the same, while the PPV values decrease when compared to the balanced prior setting. However, the maximum PPV can still go up to 90% for some runs. Thus, Merlin poses greater privacy threat than Yeom.

B Results for RCV1X

RCV1X is a 52 class classification data set consisting of Reuters news articles belonging to one of the 52 disjoint groups of similar articles. Since the number of classes is less than the other two data sets, we expect a lower attack success rate for this data set. This is in accordance with the findings of prior works Song [2017], Yeom et al. [2018].

B.1 Non-private models trained on RCV1X

We plot the distribution of per-instance loss of members and non-members for a non-private model trained on RCV1X in Figure 15a. While more members are concentrated closer to zero loss than the non-members, we observe that the gap between the two distributions is not as large as with the other two data sets. Moreover, 3628.60 ± 451.43 non-members have zero loss, and hence the

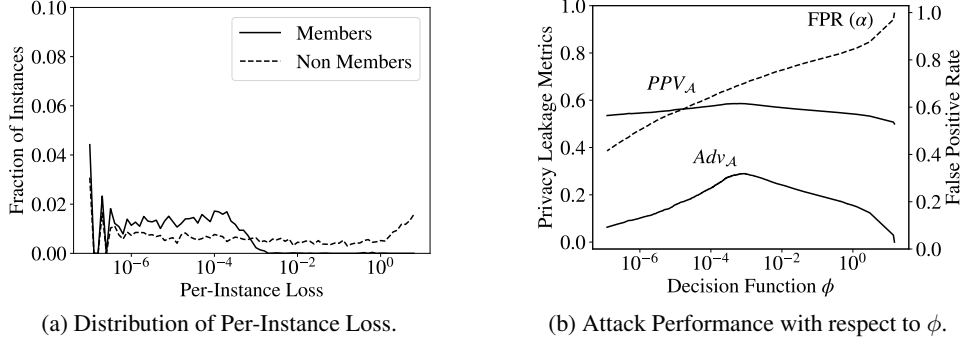


Figure 15: Analysis of Yeom on non-private model trained on RCV1X with balanced prior.

minimum possible false positive rate for Yeom is around 41% Figure 15b shows the performance of Yeom for different loss thresholds. The maximum PPV that can be achieved using this attack is only around 58%, at which point the membership advantage is close to 28%. Thus while the membership advantage metric would suggest that there is privacy risk, we can see that Yeom does not pose significant risk as PPV is close to 50% in the balanced prior setting.

Figure 16a shows the distribution of loss direction counts for a non-private model trained on RCV1X data set. The gap between the member and non-member distributions is small, however the PPV is still high with large thresholds, as depicted in Figure 16b. We repeat this experiment five times and found that the attack can achieve a maximum PPV of around 98% on an average for threshold values close to 97. Thus, Merlin poses privacy threat even in scenarios where Yeom fails.

Table 9 compares the membership inference attacks on RCV1X for different attack goals. The results suggest that Yeom is benefited from using class based thresholds, as the maximum PPV jumps from around 58% to around 93%. However, Merlin still outperforms Yeom CBT in terms of maximum achievable PPV.

B.2 Private models trained on RCV1X

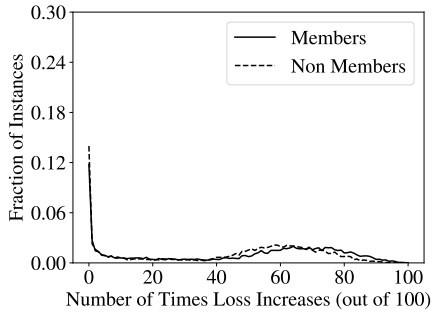
Table 10 compares the maximum PPV achieved by Yeom and Merlin attacks against private models trained on RCV1X with varying privacy loss budgets. While the privacy leakage increases with increase in privacy loss budget, neither of the attacks pose significant privacy threat. Although, Merlin still achieves higher PPV than Yeom.

Figure 17a shows the loss distribution of member and non-member records for a private model trained with $\epsilon = 100$. As shown, the gap between the two distributions is much lower when compared to Figure 15a with no privacy. Figure 17b shows the attack performance at different thresholds. Due to the reduced gap between the member and non-member loss distributions, the PPV is close to 50% across all loss thresholds. Thus small privacy noise is sufficient to mitigate privacy leakage risk.

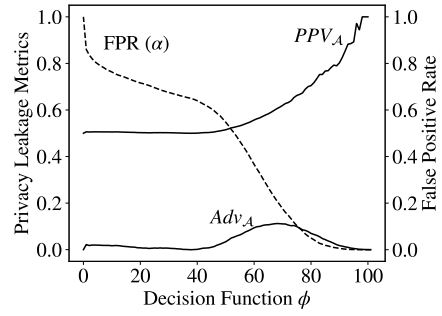
Next we plot the performance of Merlin on a private model trained with $\epsilon = 100$ in Figure 18. Figure 18a shows the distribution of loss direction counts for member and non-member records. When compared to the corresponding distribution for a non-private model (see Figure 16a), the gap between the distributions is not even noticeable. However, the attack can still achieve PPV close to 60% at higher thresholds as shown in Figure 18b. We conclude that Merlin does not pose any serious privacy risk in this setting.

B.3 Imbalanced prior setting for RCV1X

Figure 19 shows the performance of membership inference attacks across different thresholds at $\gamma = 2$ and $\gamma = 10$. As expected, the membership advantage remains unchanged for both the attacks



(a) Distribution of Increase in Loss Count.

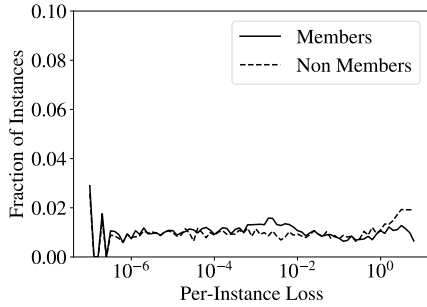


(b) Attack Performance with respect to ϕ .

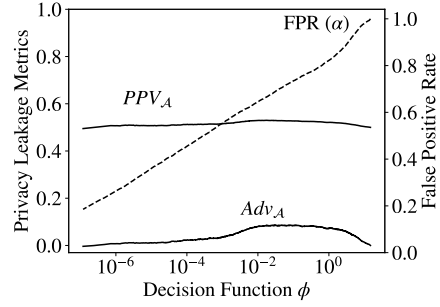
Figure 16: Analysis of Merlin on non-private model trained on RCV1X with balanced prior.

ϵ	α (%)	Yeom		Merlin		
		ϕ	Max PPV_A (%)	α (%)	ϕ (out of 100)	Max PPV_A (%)
1	20.00	$(3.09 \pm 0.69) \times 10^{-3}$	51.09 ± 0.20	1.00	82.60 ± 0.49	52.99 ± 2.09
10	55.00	$(7.93 \pm 0.08) \times 10^{-3}$	51.62 ± 0.09	1.00	83.40 ± 0.49	56.39 ± 6.55
100	65.00	$(9.93 \pm 0.88) \times 10^{-3}$	52.77 ± 0.08	1.00	84.40 ± 0.49	62.70 ± 4.29

Table 10: Membership inference attacks against private models trained on RCV1X data set with balanced prior.

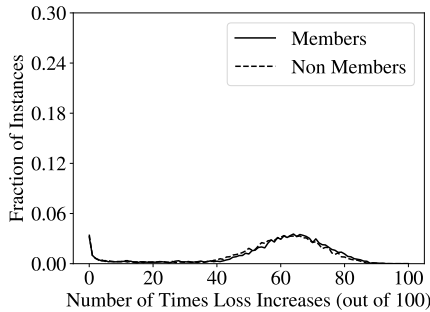


(a) Distribution of Per-Instance Loss.

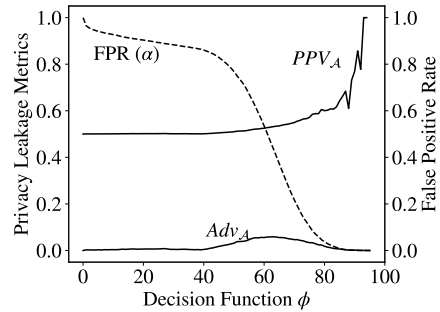


(b) Attack Performance with respect to ϕ .

Figure 17: Analysis of Yeom on private model trained with $\epsilon = 100$ at $\gamma = 1$ (RCV1X).



(a) Distribution of Per-Instance Loss.



(b) Attack Performance with respect to ϕ .

Figure 18: Analysis of Merlin on private model trained with $\epsilon = 100$ at $\gamma = 1$ (RCV1X).

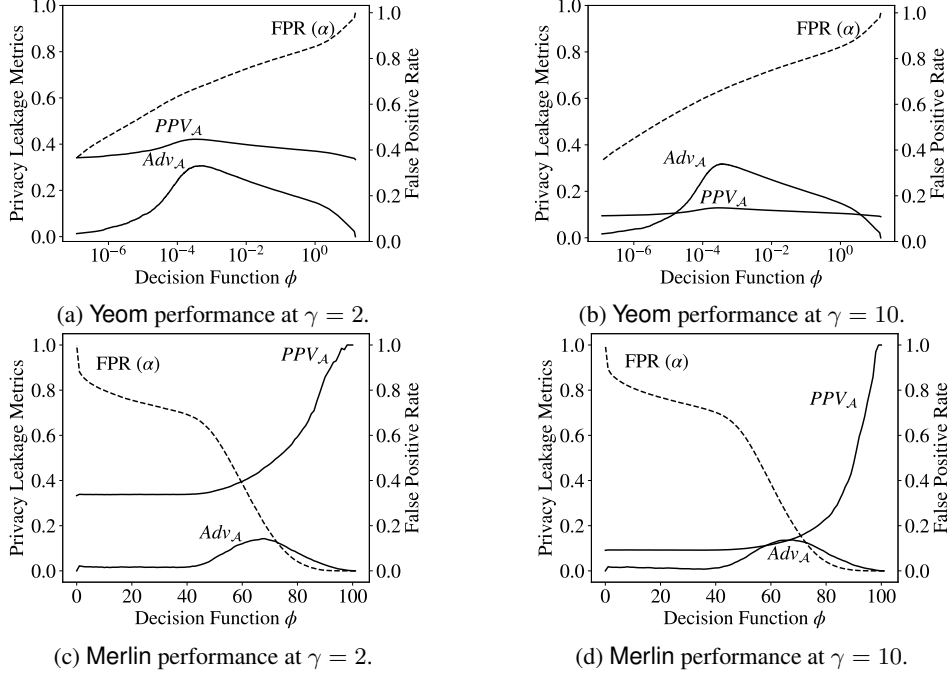


Figure 19: Attack performance on RCV1X for imbalanced prior setting.

between $\gamma = 2$ and $\gamma = 10$, since it does not consider prior probability. Whereas, we can see a drop in PPV values when we change γ from 2 to 10. The maximum achievable PPV for Yeom is 42.02 ± 0.44 at $\gamma = 2$ and 12.59 ± 0.36 at $\gamma = 10$ on an average across five runs. Thus, Yeom does not pose any privacy threat against RCV1X data set for imbalanced priors. Whereas, Merlin still seems to achieve high PPV values. We find that Merlin achieves maximum PPV of 97.10 ± 1.83 at $\gamma = 2$ and 81.23 ± 6.28 at $\gamma = 10$ on an average across five runs (as shown in Table 6). Thus, Merlin poses some privacy threat even in scenarios where Yeom fails.